ORIGINAL ARTICLE

JBMR®

Sclerostin Antibody–Induced Changes in Bone Mass Are Site Specific in Developing Crania

Amanda L Scheiber,[1,2] David K Barton,[1,2] Basma M Khoury,[1] Joan C Marini,[3] Donald L Swiderski,[4] Michelle S Caird,[1] and Kenneth M Kozloff[1,2]

[1]Department of Orthopaedic Surgery, University of Michigan, Ann Arbor, MI, USA
[2]Department of Biomedical Engineering, University of Michigan, Ann Arbor, MI, USA
[3]Bone and Extracellular Matrix Branch, National Institute of Child Health and Human Disorders, NIH, Bethesda, MD, USA
[4]Kresge Hearing Research Institute, University of Michigan, Ann Arbor, MI, USA

ABSTRACT

Sclerostin antibody (Scl-Ab) is an anabolic bone agent that has been shown to increase bone mass in clinical trials of adult diseases of low bone mass, such as osteoporosis and osteogenesis imperfecta (OI). Its use to decrease bone fragility in pediatric OI has shown efficacy in several growing mouse models, suggesting translational potential to pediatric disorders of low bone mass. However, the effects of pharmacologic inhibition of sclerostin during periods of rapid growth and development have not yet been described with respect to the cranium, where lifelong deficiency of functioning sclerostin leads to patterns of excessive bone growth, cranial compression, and facial palsy. In the present study, we undertook dimensional and volumetric measurements in the skulls of growing Brtl/+ OI mice treated with Scl-Ab to examine whether therapy-induced phenotypic changes were similar to those observed clinically in patients with sclerosteosis or Van Buchem disorder. Mice treated between 3 and 14 weeks of age with high doses of Scl-Ab show significant calvarial thickening capable of rescuing OI-induced deficiencies in skull thickness. Other changes in cranial morphology, such as lengths and distances between anatomic landmarks, intracranial volume, and suture interdigitation, showed minimal effects of Scl-Ab when compared with growth-induced differences over the treatment duration. Treatment-induced narrowing of foramina was limited to sites of vascular but not neural passage, suggesting patterns of local regulation. Together, these findings reveal a site specificity of Scl-Ab action in the calvaria with no measurable cranial nerve impingement or brainstem compression. This differentiation from the observed outcomes of lifelong sclerostin deficiency complements reports of Scl-Ab treatment efficacy at other skeletal sites with the prospect of minimal cranial secondary complications. © 2019 American Society for Bone and Mineral Research.

KEY WORDS: SCLEROSTIN ANTIBODY; OSTEOGENESIS IMPERFECTA; CRANIAL MORPHOLOGY; ANABOLIC EFFECT; VASCULARITY

Introduction

Osteogenesis imperfecta (OI) is a genetic disorder caused by collagen-related mutations, resulting in brittle bones, high fragility rates, and associated skeletal deformities.[1] Pharmacologically, pediatric OI is primarily managed with bisphosphonates, which work as osteoclast inhibitors to reduce high bone turnover as well as modify bone size and shape due to disruptions in modeling-associated growth.[2,3] Currently the only approved anabolic therapies for bone formation act by signaling through the parathyroid hormone receptor,[4,5] which cannot be utilized to treat pediatric individuals because of potential side effects.[6,7] Thus, there is room for development of anabolic treatment options to support bone formation for therapy of pediatric OI.

Sclerostin is an osteocyte-specific glycoprotein that negatively regulates bone formation by blocking canonical Wnt signaling.[8] Sclerostin antibody (Scl-Ab) therapy has emerged as a potential means to interfere with sclerostin and thus increase bone formation. It has been shown to increase bone mass in clinical trials of adult diseases of low bone mass, such as osteoporosis[9] and OI.[10] Its use to decrease bone fragility in pediatric OI has been evaluated in several growing mouse models by us and others, and significant gains in cortical and trabecular bone mass at non-cranial sites during periods of rapid bone growth have been reported.[10–14] At cortical bone sites, we previously demonstrated that Scl-Ab is capable of changing quiescent and resorbing surfaces into bone formation surfaces, leading to decrements in whole-bone fragility.[15] Enhancing bone deposition could be beneficial to pediatric individuals with OI; however, loss of resorbing surfaces could

Received in original form September 18, 2018; revised form July 24, 2019; accepted August 14, 2019. Accepted manuscript online August 23, 2019.
Address correspondence to: Kenneth M Kozloff, PhD, Department of Orthopaedic Surgery, 2015 BSRB, 109 Zina Pitcher Place, Ann Arbor, MI 48109-2200, USA.
E-mail: kenkoz@umich.edu
Additional Supporting Information may be found in the online version of this article.
Journal of Bone and Mineral Research, Vol. 34, No. 12, December 2019, pp 2301–2310.
DOI: 10.1002/jbmr.3858

also pose a risk that is unique to this population. Localized resorption is critical to reshaping bones during growth; in the skull such remodeling is critical for growth of the brain, nerves, and blood vessels. Anomalies associated with lifelong sclerostin deficiency or loss of function, such as that observed in patients with sclerosteosis or Van Buchem disease, may predict some of the potential risks of utilizing Scl-Ab-mediated therapy in a developing pediatric population.

Patients with lifelong deficiency in sclerostin demonstrate patterns of excessive bone growth resulting in cranial nerve compression and facial palsy associated with nerve impingement.[16,17] The most perilous morphological change observed in crania of patients with Van Buchem's disease is narrowing of the foramen magnum, which can result in sudden death due to compression of the brain stem.[18] Patients heterozygous for sclerostin deficiency or loss of function do not show similar deleterious outcomes,[19] suggesting a gene-dosing effect with potential translation to pharmacologic inhibition of sclerostin during growth and development.

Individuals with OI have unique skull morphology that may impact Scl-Ab-associated changes. Because of OI, the cranium is often abnormally shaped,[20] and, in some forms of OI, individuals demonstrate abnormally thin skulls.[21] Although rare, prominent occipital regions or flattening of the cranial vault may occur.[22] A common radiographic indicator of OI is the presence of Wormian bones, accessory skull bones completely surrounded by a suture line.[23] These abnormal ossicles are frequently found in individuals with OI due to reduced skull ossification.[24] Murine cranial development has been used extensively to evaluate genetic impact on human cranial bone development, and 3D micro-CT has been assessed to validate the mouse cranium as a relevant model for clinical features of OI[25] and other genetic disorders.[26] Although Scl-Ab has been explored in many simulated disease models of low bone mass resulting from ovariectomy,[27,28] orchidectomy,[29] glucocorticoid exposure,[30] disuse,[31,32] spinal cord injury,[33] rotator cuff healing,[34] and fracture repair,[35,36] these studies and others were typically performed in mature animals where most cranial developmental processes are complete. Similarly, in studies of young OI mice, the effects of pharmacologic sclerostin inhibition on the cranium during periods of rapid growth and development have not yet been described.[10,12–15] These outcomes may have significant implications in determining the safety of Scl-Ab for treatment of low bone mass in pediatric populations.

The purpose of this study was to determine the morphological changes in the developing crania induced by Scl-Ab. To assess this, the Brtl/+ (HET) mouse model of OI[37–39] was treated with Scl-Ab throughout a period of rapid growth. Cranial morphology was assessed by micro-CT at multiple sites to determine the influence of sclerostin inhibition on modulation of bone mass.

Materials and Methods

Treatment design and functional assessment

As part of a larger dose–response study, male Brtl/+ and wild-type (WT) mice were administered one of five doses of Scl-Ab VI (3, 6, 12.5, 25, 50 mg/kg, Amgen, Thousand Oaks, CA, USA, and UCB, Brussels, Belgium) and compared with saline-injected controls (n = 10/group). Doses were administered subcutaneously biweekly, from age 3 to 14 weeks. Previously, we have demonstrated that biweekly administration of 25 mg/kg Scl-Ab induced significant therapeutic benefits in femora of Brtl/+ between 3 and 8 weeks of age.[10,40] In the present study, we chose Scl-Ab dose and durations to double our prior treatment exposure to better understand the outcomes of a maximal, sustained effect of treatment throughout growth. Animals were housed in specific pathogen-free cages with standard 12-hour light/dark cycles with *ad lib* access to food and water. All studies were approved by the University of Michigan Institutional Animal Care and Use Committee (IACUC). At 8 and 13 weeks of age, mice were assessed for symptoms characteristic of Bell's palsy, a facial paralysis that could indicate facial nerve compression, by puffing air across the eyes to assess the blink reflex, and by assessing asymmetry in mouse whisker movement following previously described protocols.[41] After euthanasia by CO_2, skulls were dissected and preserved for micro-CT by fixing in 10% NBF and subsequently stored in 70% ethanol.

Micro-CT imaging

To assess the extreme Scl-Ab-induced conditions that might lead to morphological changes in the skull, crania from mice treated with the maximum dose of 50 mg/kg were compared with the control group. To verify whether Scl-Ab dose impacts the extent of morphological changes, locations that exhibited significant morphological changes were also analyzed in mice treated with intermediate doses of 25 mg/kg. To compare the extent of dimensional changes caused by Scl-Ab in relation to changes observed during growth, additional crania of untreated mice at 3 weeks of age were dissected, scanned, and analyzed.

Crania were imaged using micro-computed tomography (Skyscan 1176, Bruker, Kontich, Belgium) at 9-micron voxel size. Scan parameters included a 0.3° increment angle, 2 frames averaged, 65-kVp and 385-μA X-ray source with a 1-mm Al filter to reduce beam hardening artifacts.

Dimensional shape analysis

To test for deformations in the mouse crania similar to those found in individuals with OI, spatial coordinates of the nasale, nasion, bregma, lambda, the intersection of interparietal and occipital bones (IP/OP) at the midline, and the intersection of parietal, temporal, and interparietal bone (PTI) were found using commercially available software (Dragonfly 3.0, Object Research Systems, Montreal, Canada) (Fig. 1*A*, *B*). Using these coordinates, distances between anatomic landmarks and the angles between those segments were computed (Table 1) using protocols adapted from Richtsmeier and colleagues.[42] Distances and angles such as these are highly inter-correlated with each other, making individual statistical testing difficult.[43] To better control for this, we used geometric morphometric methods[44,45] implemented in the R package Geomorph[46] to assess variation in shape (ie, the relative positions of the landmarks, which encompass both the relative lengths of all inter-landmark distances and the angles between those segments). By treating each set of landmarks as a single configuration, with a single shape, a measure of the magnitude of shape distance (Proscrutes distance) was created. Differences between shapes can be illustrated visually by deformation grids,[47] while trajectory analysis[48] can then be used to determine overall statistical relevance. Trajectory analysis was used to compare vectors connecting selected group means, in this case, untreated WT versus untreated Brtl/+ for genotypic assessment, and untreated WT to treated Brtl/+ for rescue effect.

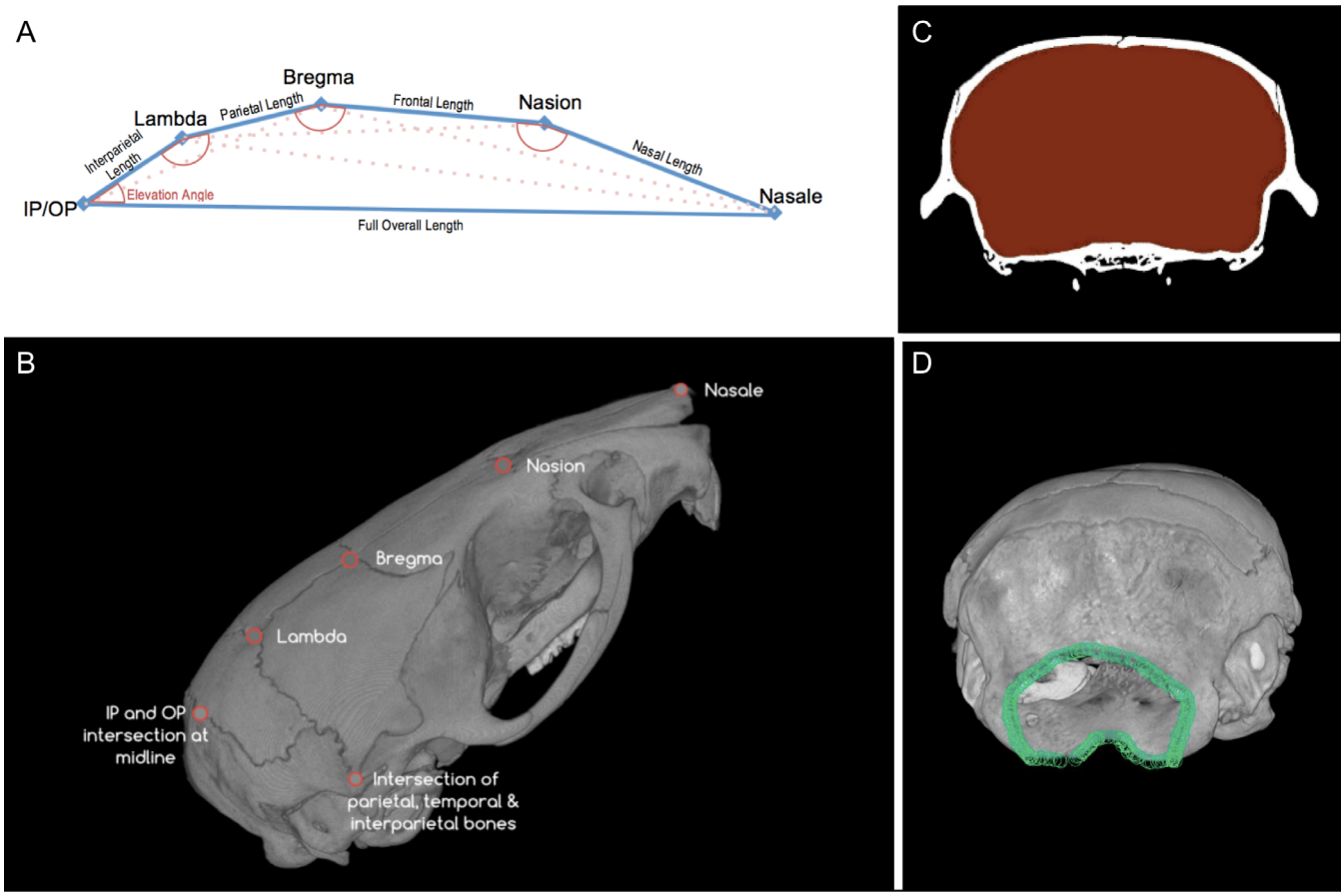

Fig. 1. (*A*) Landmark locations and calculated values. (*B*) Landmark locations measured on exertior of crania. (*C*) Sample region of interest obtained for intracranial volume. (*D*) Sample foramen magnum outline.

Table 1. Measured Values and Landmarks Used

Measurement	Landmarks used
Length	
Mean cranial length	IP/OP, nasale
Mean interparietal length	IP/OP, lambda
Parietal length	Lambda, bregma
Frontal length	Bregma, nasion
Nasal length	Nasion, nasale
Angle	
Mean interior angle at lambda	IP/OP, lambda, bregma
Mean interior angle at bregma	Lambda, bregma, nasion
Mean interior angle at nasion	Bregma, nasion, nasale
Mean interior lateral angle	IP/OP, PTI, perpendicular
Mean interior elevation angle	Lambda, IP/OP, nasale

IP/OP = interparietal and occipital bones; PTI = parietal, temporal, and interparietal bones.

Suture morphology

Suture interdigitation plays a critical role in developing a connection between calvarial bones, resisting mechanical tension.[49,50] Wnt signaling plays an important role in suture development[51] and suture morphology and interdigitation that evolves during growth and development.[52] To quantify the effects of genotype and on the complexity of cranial sutures, the parietal suture was traced from the bregma to lambda at 45-micron intervals. Coordinates were analyzed based on the sum of deviation of distance from a normalized midline.

Calvarial thickness analysis

To evaluate the effect of Scl-Ab on skull thickness, the thicknesses of the parietal bone was calculated using measurement and visualization software (CTAn, Bruker), by creating a region of interest through transverse slices around the entire parietal bone from the lambda to bregma. A region of interest was created within the cranium for every transverse slice from the nasion to the foramen magnum (Fig. 1*C*); total intracranial volume was also calculated using the same software.

Foramen analysis

The effects of treatment on size were evaluated for the interpterygoid foramen, foramen ovale, anterior ethmoidal foramen, anterior lacerated foramen, stylomastoid foramen, and anterior semicircular auditory canal. Such locations were selected because of their consistent cylindrical structure, diverse physiological purpose, and variation in cross-sectional diameter and involvement in sclerosteosis. To determine whether changes in vascular foramina are unique to the skull, the basivertebral

foramen in the 5th lumbar vertebra was included in the study. Automatic thresholding through CTAn was applied to each region of interest and average cross-sectional areas orthogonal to foramina orientation were obtained for each site, utilizing local landmark locations to ensure consistency. A similar technique was applied to the apex of the semicircular canal.

Because the foramen magnum has a complex, three-dimensional shape, a single planar projection would not suffice to capture changes in the magnitude of this opening. Instead, the three-dimensional outline of the foramen magnum was constructed using the outlining coordinates at a 9-micron interval for each specimen (Fig. 1*D*). The three-dimensional centroid of this outline was calculated, and the size of the foramen was calculated as the square root of the sum of coordinates' distances from the centroid.

Statistical interpretation

Before statistical analysis, data were linearized. This transformation included taking the natural log of the square and cube root of area and volumetric measurements, respectively. Statistical analysis of effects of genotype and treatment on shape was performed on the full set of foramina. A two-way multivariate ANOVA was used to test for differences between average cross-sectional areas of foramina.

Statistical comparisons among the genotype, control, and treated groups were made using a multiple regression two-way ANOVA, considering $p < 0.05$ as significant. Post hoc analysis was conducted utilizing a Welch two-sample t test when interaction was present or to evaluate for type-1 error. Further analysis also included a comparison of Brtl/+ Scl-Ab to the WT vehicle group, evaluating Scl-Ab's ability to provide restorative anabolic gains.

Results

Genotype has modest influence on skull shape

Deformed grid illustrations of the skull at 14 weeks suggest that untreated Brt/+ tend to have a more domed skull than WT, with parietal and nasal regions expanded relative to the rest of the skull (Fig. 2*Ai*). To confirm the visual impressions obtained from examination of the deformed grids, we quantified changes in the lengths and angles that appeared to be most strongly affected (Table 2, Fig. 3). These analyses confirm that the frontal bone is shorter in untreated Brtl/+ than in WT, whereas the other cranial bones are longer in untreated Brtl/+ than in WT (Table 2, Fig. 3*B*, *C*, *E*). A larger, straighter lambda angle and smaller, sharper bregma angle in Brtl/+ contribute to the phenotype of a higher-crowned, more domed appearance (Table 2, Fig. 3*F*, *G*). The net effect of these individual changes is to maintain a stable total length for the whole skull and for the calvarium despite differences in the individual components comprising those measurements. Statistical assessment of vectors to untreated Brtl/+ from untreated WT confirms that the effect of OI on overall cranial shape in these mice is quite small (Fig. 2*B*).

Scl-Ab influences cranial shape

Small differences between average cranial shapes suggest that Scl-Ab may have a weak effect on the way that OI alters skull

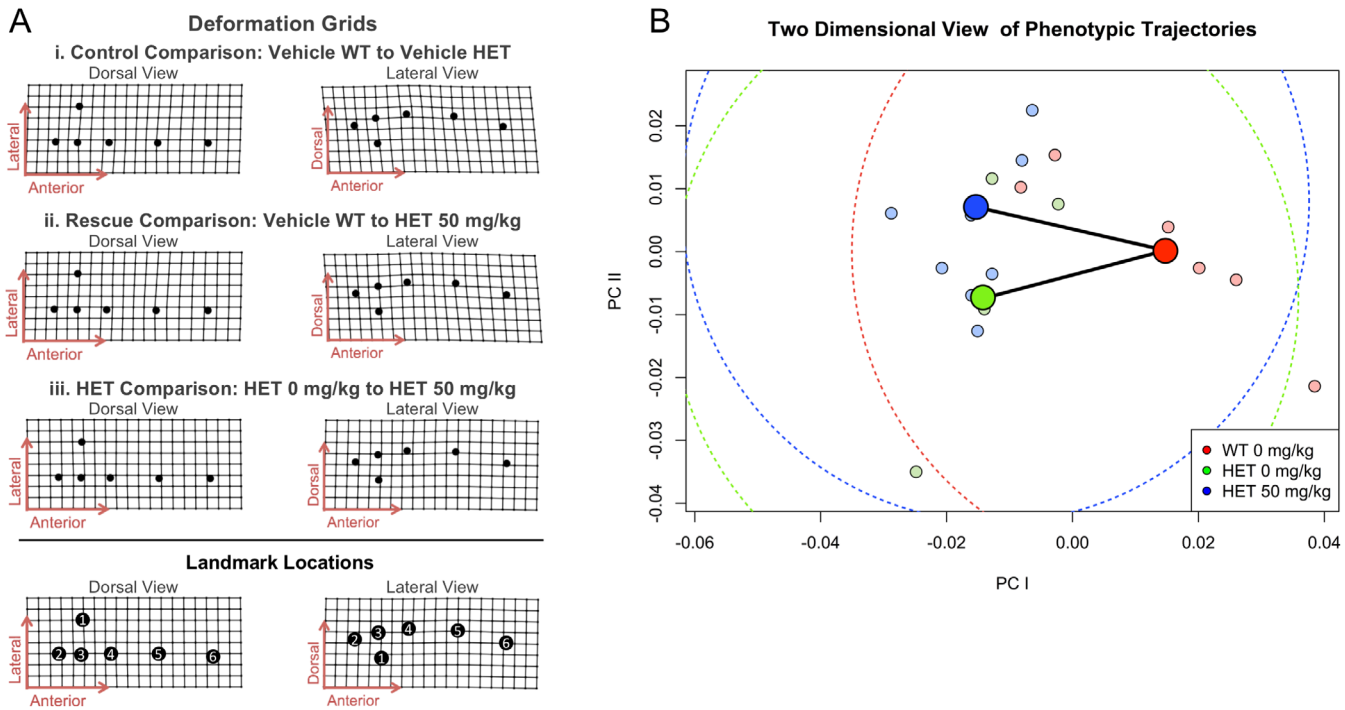

Fig. 2. (*A*) Dorsal and lateral views of deformations for three pairwise group differences. Landmark locations are identified in reference view. 1) PTI; 2) IP/OP; 3) lambda; 4) bregma; 5) nasion; 6) nasale. (*B*) Trajectory analysis demonstrates a statistically insignificant difference between veh WT (red), veh HET (green), and treated HET (blue) mean shapes. Lightly colored points represent individual measurements; darker points are means of each group. Dashed curves represent radii of statistical difference between groups.

Table 2. Mean Length and Angle Measurements (Genotype Percent Changes Compares WT to HET; Scl-Ab Treatment Percent Change Compares 0 mg/kg to 50 mg/kg)

	HET 0 mg/kg	HET 50 mg/kg	WT 0 mg/kg	WT 50 mg/kg	Genotype	Scl-Ab treatment
Length (mm)						
Mean cranial length	21.21 ± 0.55	21.58 ± 0.39	21.53 ± 0.57	22.16 ± 0.39	−2.06%	2.34%
Mean interparietal length	2.68 ± 0.47	2.75 ± 0.53	2.50 ± 0.34	2.47 ± 0.20	9.26%	0.77%
Parietal length	4.44 ± 0.56	4.21 ± 0.36	4.07 ± 0.19	3.87 ± 0.18	8.94%	−5.05%
Frontal length	6.77 ± 0.34	6.94 ± 0.30	7.36 ± 0.20	7.66 ± 0.12	−8.72%	3.33%
Nasal length	7.16 ± 0.11	7.47 ± 0.26	6.80 ± 0.72	7.44 ± 0.29	2.74%	6.81%
Angle (radian)						
Mean interior angle at lambda	2.85 ± 0.09	2.86 ± 0.12	2.76 ± 0.04	2.75 ± 0.04	3.63%	0.00%
Mean interior angle at bregma	2.96 ± 0.03	2.97 ± 0.06	3.05 ± 0.03	3.03 ± 0.04	−2.47%	−0.17%
Mean interior angle at nasion	2.98 ± 0.03	2.94 ± 0.03	2.93 ± 0.05	2.89 ± 0.04	1.72%	−1.35%
Mean interior lateral angle	0.33 ± 0.05	0.32 ± 0.05	0.30 ± 0.02	0.32 ± 0.02	4.84%	1.59%
Mean interior elevation angle	0.26 ± 0.02	0.23 ± 0.03	0.28 ± 0.05	0.27 ± 0.05	−10.91%	−7.41%

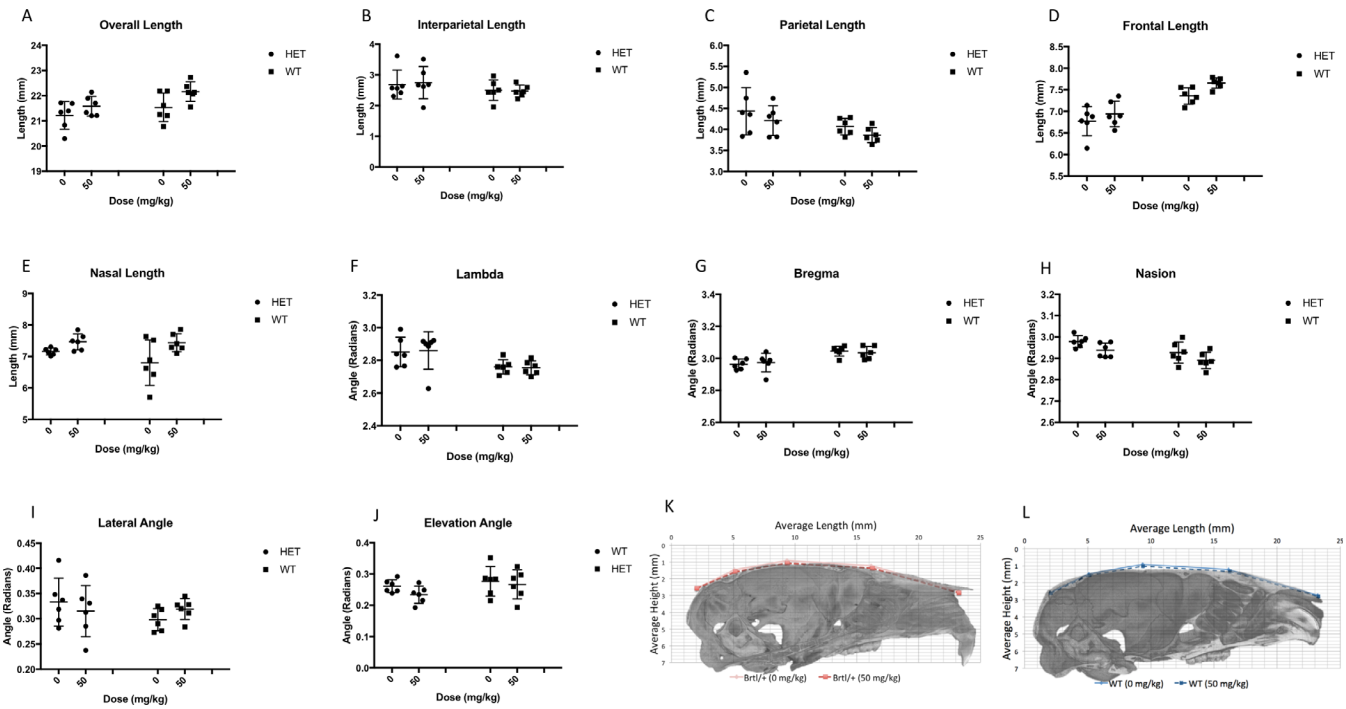

Fig. 3. Micro-CT data from cranial landmark measurements demonstrate genotype and Scl-Ab effect on cranial lengths (*A–E*) and (*F–J*) on cranial angles. Superimposed mean lengths and angles of crania for (*K*) Brtl/+ and (*L*) WT mice. Data are shown as mean ± SEM of measurements.

growth (Fig. 2). Treated Brtl/+ also differed from untreated WT in having a more domed skull, with similar relative elongation of the parietal and nasal (Fig. 2*Aii*), but with more flexion of the nasal than in untreated Brtl/+ (Fig. 2*Aiii*). As shown in the plane of the first two PCs of the data (Fig. 2*B*), the distributions of the three groups overlap broadly, and vectors to treated and untreated Brtl/+ from WT are not significantly different, indicating the differences between overall skull shapes are small relative to within-group variation.

Parietal thickness increases with Scl-Ab treatment, rescuing the genotypic deficit

Parietal thickness is strongly influenced by both genotype ($p < 0.0001$) and treatment ($p < 0.0001$) (Fig. 4*A*). Brtl/+ have 23.6% thinner parietal bones than WT. Treatment with 25 mg/kg Scl-Ab eliminated that difference ($p = 0.99$). Representative calvarial cross sections from both Brtl/+ and WT mice are shown in Fig. 4*B*.

Intracranial volume is not impacted by Scl-Ab despite genotypic differences

These more domed, thinner calvarial bones found in Brtl/+ resulted in a 7.6% smaller intracranial volume compared with WT mice ($p = 0.002$) (Fig. 4*A*). Although Scl-Ab induced significant calvarial thickening, intracranial volume was more strongly influenced by overall patterns of skull shape. Accordingly, there were no significant differences in intracranial volume between the control and treatment groups for either Brtl/+ and WT mice ($p = 0.88$).

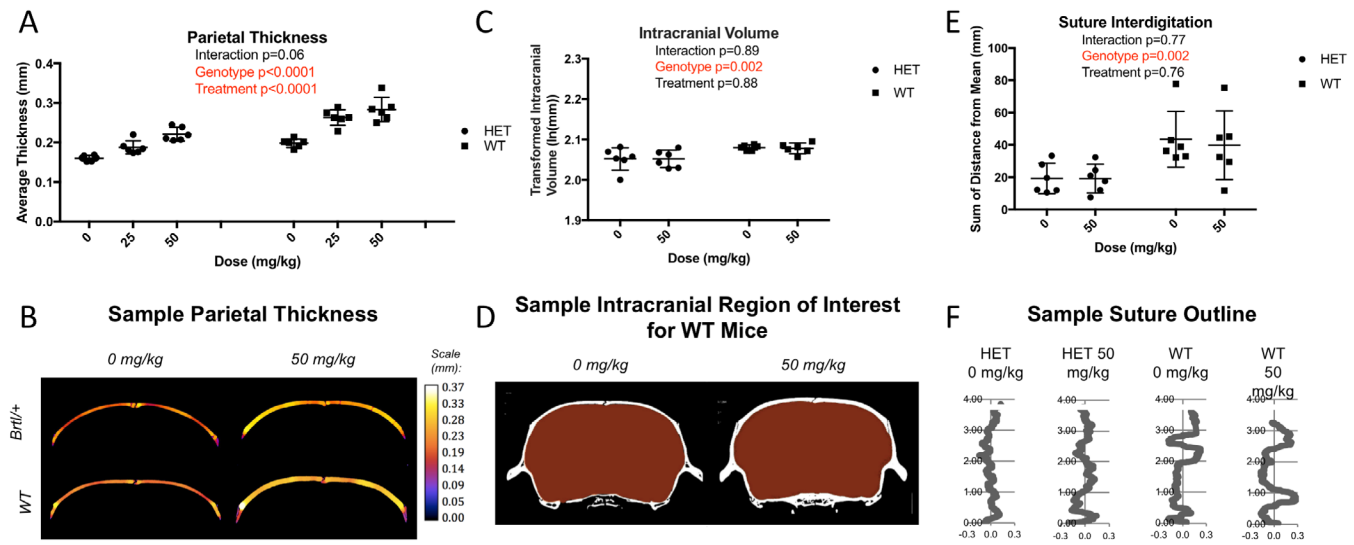

Fig. 4. (*A*) Micro-CT data of the parietal bone reveals average parietal thickness is impacted by genotype and treatment. (*B*) Sample parietal thickness regions of interest. Color look-up scale represents the measured thickness at each location in mm using local thickness computation. (*C, D*) Micro-CT imaging reveals intracranial volume is impacted by genotype but not SclAb treatment. (*E*) Micro-CT data of the parietal suture reveal interdigitation is impacted by phenotype but not Scl-Ab treatment. (*F*) Sample suture outlines demonstrate interdigitation differs between genotype but is not impacted by Scl-Ab. Data are shown as mean ± SEM of measurements.

Scl-Ab does not influence suture interdigitation

The midline parietal suture of Brtl/+ mice has 53.9% less interdigitation (smaller mean squared deviation from the midline) than in WT mice ($p = 0.002$) (Fig. 4*E*). Scl-Ab treatment had no effect on suture interdigitation in both Brtl/+ and WT mice ($p = 0.76$). Representative images of the morphologic tracings of sutures from each experimental group are shown in Fig. 4*E*. No Wormian bones were observed on any of the sutures.

Table 3. Foramen Multivariate Analysis of Variance (MANOVA) Results

Factor	Pillai's trace	Approximate *F* value	*p* Value
Treatment	0.865	12.761	<0.001
Genotype	0.533	2.284	0.089
Treatment and genotype	0.254	0.681	0.686

Scl-Ab induces few changes in cross-sectional areas of passages through cranial bones

Multivariate analysis of all six cranial foramina that were examined indicated a significant effect of treatment but only a marginal effect of genotype (Table 3). There was not a significant interaction, thus the effect of treatment was not influenced by genotype. In post hoc analyses of the individual foramina, only the foramen ovale differed significantly between genotypes, being larger in Brtl/+ (Fig. 5). With respect to Scl-Ab treatment, the interpterygoid foramen, which is a venous passage,[53] showed significant, dose-dependent decrease in size in both genotypes (Fig. 5*F*). However, there was no indication that cranial foramina with nerve functions had similar narrowing effects with treatment. The foramen ovale, anterior lacerated foramen, and stylomastoid foramen all function as nerve passages[54] whereas the anterior ethmoidal foramen serves as a passageway for the internal ethmoidal artery, vein, and nerve[55] and neither these nor the foramen magnum were affected by genotype ($p = 0.63$) or treatment ($p = 0.25$) (Fig. 5). Consistent with these results, no mice exhibited changes in blink or whisker responses that would indicate facial nerve compression.

Similar to the interpterygoid foramen, the basivertebral foramen, an extracranial postnatal foramen with strictly vascular function[56] exhibited substantial constriction in treated mice (61.0% smaller, $p = 0.0003$).

Interestingly, the cross-sectional area of the anterior semicircular canal, a fluid-filled segment of the inner ear that is critical for coordinating eye movement with head movement and which does not differ between genotypes ($p = 0.28$), was 16.1% larger in treated than in untreated mice ($p = 0.005$) (Fig. 6*A*).

Behavioral analyses confirmed no effect of Scl-Ab

Assessment of blink and whisker reflexes after 5 and 10 weeks of treatment (8 and 13 weeks of age) were unremarkable across genotypes. No changes were observed over time or bilaterally, with no overt functional deficiencies that would be suggestive of significant nerve impingement as a consequence of bone overgrowth or resulting from genotypic differences between mice.

Twenty-one-day-old crania demonstrate the extent of growth-related dimensional changes observed during treatment

To compare the extent of dimensional changes caused by Scl-Ab treatment in relation to the changes observed during growth over the treatment period, 21-day-old (21D) cranial morphology

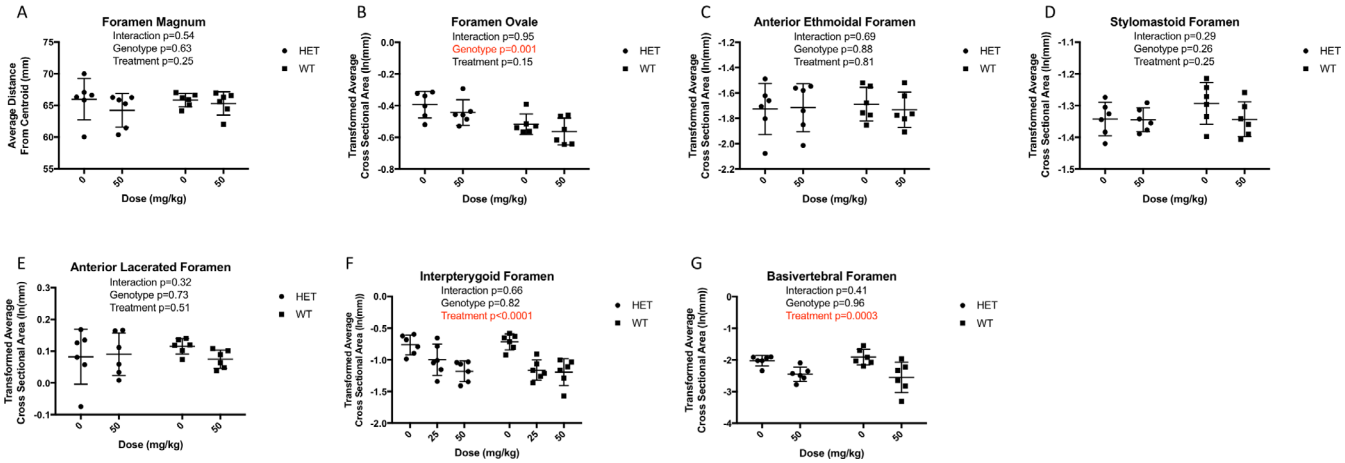

Fig. 5. Micro-CT average cross-sectional measurements of foramen reveal the interpterygoid is the only foramen impacted by Scl-Ab (*A–F*), despite genotypic differences (*G*). Micro-CT of basivertebral foramen reveal Scl-Ab induces changes in average cross-sectional area. Data are shown as mean ± SEM of measurements.

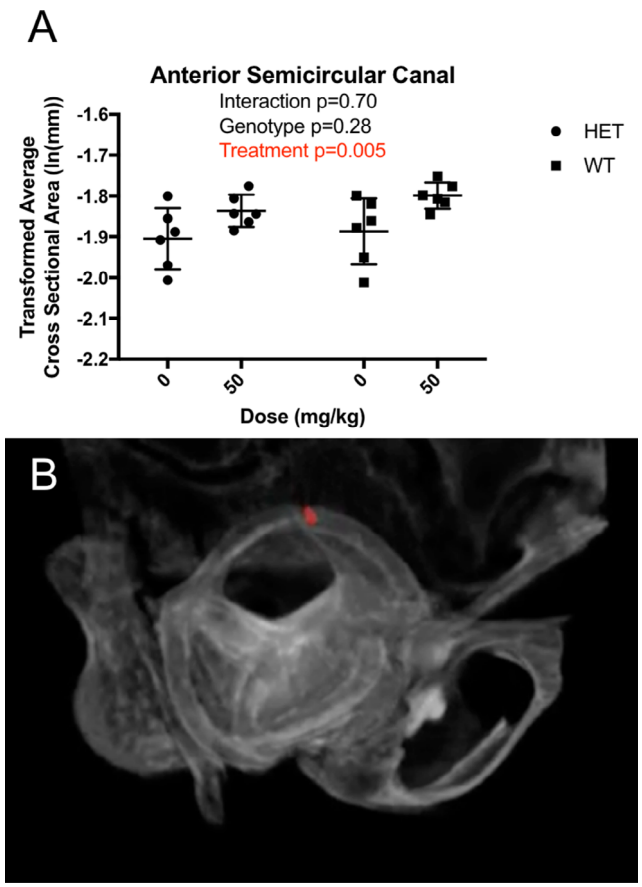

Fig. 6. Micro-CT average cross-sectional measurements of the anterior semicircular canal reveals (*A*) Scl-Ab causing an increase in cross section, with no impact by phenotype. (*B*) Sample region of interest measured. Data are shown as mean ± SEM of measurements.

was measured in a manner consistent with aged samples (Supplemental Fig. S1). To calculate and compare growth percent, each group at 14 weeks (ie, Scl-Ab and Veh for both genotypes) was compared within genotype to corresponding 21D values.

The alterations in growth prompted by Scl-Ab treatment are minor in comparison to the overall growth that occurs naturally during the treatment period (Supplemental Fig. S1). When compared with 3-week controls, overall cranial lengths of Brtl/+ and WT Veh expanded by 14.9% and 13.5%, respectively, over 21D values. Scl-Ab-treated animals showed a growth of 16.9% (Brtl/+) and 16.7% (WT) over 21D values, reflecting minimal differences in growth patterns with the addition of Scl-Ab. Similarly, Scl-Ab induced minor changes in growth from 21D compared with Veh-treated growth patterns over the same period in the frontal (Brtl/+ Veh: 11.0% versus Scl-Ab: 13.8%; WT Veh: 13.8% versus Scl-Ab: 18.4%), and nasal (Brtl/+ Veh: 42.1% versus Scl-Ab: 48.2%; WT Veh: 8.4% versus Scl-Ab: 16.5%) lengths. Treatment effects in relation to growth effects are further summarized in Supplemental Fig. S1. Similar modest effects of Scl-Ab on growth with respect to angular changes in the crania are summarized in Supplemental Fig. S2.

Because of the early developmental stage, we were unable to isolate individual foramina in 21D crania at the resolution used for micro-CT imaging.

There is a significant difference between the parietal thickness of all control and treatment groups and the 21D crania ($p < .001$) (Supplemental Fig. S3). Unlike the relatively minor changes in skull lengths and angles, the increase in parietal thickness due to treatment with Scl-Ab is significantly modified to levels closer to the increase in thickness that occurs during normal development alone. Compared with the corresponding 21D genotype, at 14 weeks the parietal thickness of Brtl/+ and WT Veh increased by 117.5% and 145.2%, respectively, whereas treatment with 25 mg/kg of Scl-Ab provoked growth by 154.6% (Brtl/+) and 225.3% (WT). Similarly, 50 mg/kg of Scl-Ab induced a growth of 199.8% (Brtl/+) and 250.6% (WT) versus 21D thicknesses.

Discussion

The purpose of this study was to determine whether Scl-Ab administration induces morphological changes in the developing crania. Through this study, several phenotypic differences

between Brtl/+ and WT cranial attributes were observed. Brtl/+ mice showed a modestly domed appearance with significant reductions in calvarial thickness versus WT, consistent with clinical observations of abnormally thin skulls.[21] Calvaria were sensitive to the treatment effects of Scl-Ab, which was capable of rescuing this deficit. Gains in calvarial thickness were consistent with our previously described gains in femora cortical thickness in Brtl/+, confirming Scl-Ab treatment effect occurs as expected in the cranium as well as long bone sites.[10] Differences in cranial lengths and angles showed trends toward minor effects with Scl-Ab; however, these did not impact overall morphology in comparison to the magnitude of response observed in parietal thickness and effects due to growth. With treatment, cranial volume was preserved, suggesting that Scl-Ab does not induce intracranial compression to the extent observed clinically with homozygous genetic deficiencies of sclerostin. Expansion of the anterior semicircular canal due to Scl-Ab was unexpected and may be an indication that other morphological changes occurred in the inner ear that might affect balance or hearing.

Narrowing of foramina occurred in two locations that function as vascular passageways but did not occur in important neural foramina, including the foramen magnum, foramen ovale, anterior ethmoidal foramen, stylomastoid foramen, and anterior lacerated foramen. The narrowing of the basivertebral foramen extended this observation to a non-cranial site, but the absence of similar responses in other foramina that included both nerve and vasculature (anterior ethmoid foramen) clouds possible explanations. One possible factor may be osteocyte proximity to affected sites. Because osteocytes are predominantly responsible for synthesizing sclerostin, the proximity or quantity of osteocytes in defined regions could restrict the effect of treatment to sites of substantial sclerostin secretion. Alternatively, a neural self-protection effect may limit Scl-Ab effects at these sites; similar self-protection effects may maintain critical vascular passages but not the foramina that pass small and variable members of venous plexuses. Although not characterized directly in these studies, local mechanical differences between foramen that permit vascular perfusion versus those dedicated to nervous innervation may induce local differences in sclerostin expression, which may influence the local anabolic response. The anabolic actions of Scl-Ab have been shown to be heightened in normally loaded bones compared with those with reduced mechanical loading in some[31,32] but not all studies.[57]

The implications of these findings of narrowing in some but not other foramina are unclear. A leading concern for pharmacologic inhibition of sclerostin during growth and development is that treatment may phenocopy intercranial pressure, nerve entrapment, and facial deformities present in patients with lifelong sclerostin deficiency.[16–18] Functional nervous changes were not observed, and foramen functioning exclusively as nervous passages were not narrowed. In patients with sclerosteosis, increased intracranial pressure can occur from reduced intracranial diameter, calvarial thickening, and jugular vein occlusion.[19] In the present study, these findings were limited to some vascular foramen occlusion, whereas intracranial volumes and shapes remained unchanged. The present findings demonstrate outcomes after a high dose for an extreme duration and suggest need for additional studies to better understand how this finding could be mitigated through a less severe treatment regimen or when Scl-Ab is combined with an antiresorptive,[58,59] possibly facilitating reduced drug exposure from both medications.

This study has several limitations. Accuracy of our measurements is dependent on our 9-micron scanning resolution. To account for this restraint, we investigated a variety of foramina that spanned multiple orders of magnitude in size. Larger foramina provided us with a reference point that was less sensitive to scanning resolution. Facial palsies resulting from nerve compression are observed in patients with both osteoblastic[16,60,61] and osteoclastic[17] defects, and Scl-Ab has known anabolic and antiresorptive effects.[9,10] Micro-CT imaging revealed site-specific structural changes in response to Scl-Ab but cannot differentiate the cellular mechanisms involved. Because of technical limitations that prevented us from matching histologic sectioning planes to micro-CT locations across the skull, we were unable to differentiate antiresorptive from anabolic actions at these sites and acknowledge the need for future studies to derive these parameters at sites that were both responsive and resistant to Scl-Ab. We were also limited to the phenotype of our Brtl/+ mouse model. Untreated Brtl/+ deviated greatest from WT with reduced calvarial thickness and intracranial volume, whereas differences in overall size and shape of the skull were more modest, reflecting some but not all craniofacial features of OI. OI is a highly variable disease; different types of collagen mutation can lead to a range of symptoms and responses to treatment. Therefore, the preliminary results from this study may not be fully reflective of all OI conditions and do not fully elucidate a direct cellular mechanism for our findings. The present study suggests a similarity of action independent of genetic mutation in the most prominent phenotypic features—calvarial thickness and intracranial volume. Whether similar treatment responses would occur across multiple OI models remains unknown and contributes to the need for the field to better understand diverging outcomes in this disorder.[62]

Our study was initially designed to examine the effect of Scl-Ab over a period of rapid long-bone growth.[10] However, approximately 80% of overall cranial growth in mice occurs during 7 to 14 days of age.[63] We began treatment of mice at age 21 days, which developmentally corresponds to a human age of approximately 2 years based on overall central nervous system and reproductive development.[64] As the majority of the cranial development occurs before this period,[65] we may have missed earlier phases of cranial growth regulated differentially by Scl-Ab. The present findings should be considered in the context of these developmental milestones.

Scl-Ab has been shown to increase bone mass in adult individuals with OI, and based on promising preclinical mouse models of the disorder[8,10,11,14,15] is proposed as a novel therapy for pediatric use. Lifelong genetic depletion of functional sclerostin can result in craniofacial abnormalities, and reports to date have not described whether sclerostin inhibition phenocopies these traits when administered during periods of growth and development. In the present study, phenotypic calvarial thinning was rescued, while abnormalities reminiscent of sclerosteosis or Van Buchem disorder including cranial compression and nerve impingement were not observed in this study. These findings likely reflect the difference between the temporary action of Scl-Ab therapy initiated at age 3 weeks in mice versus patients with a lifelong deficiency of functional sclerostin during cranial bone growth and development. This differentiation from the observed outcomes of

lifelong sclerostin deficiency complements reports of Scl-Ab treatment efficacy with the prospect of minimal cranial secondary complications.

Disclosures

KMK has received consultant fees from Mereo Biopharma. All other authors report no conflicts of interest.

Acknowledgments

The authors gratefully thank Dr David Kohn, Carol Whitinger, Rob Goulet, and Rebecca Falzon for technical assistance and thoughtful discussion. Scl-Ab was provided by Amgen (Thousand Oaks, CA, USA) and UCB (Brussels, Belgium). Research funding was provided by NIH (RO1AR062522, P30AR069620, S10 OD017979-01A1).

Authors' roles: Study designed and conducted by KMK, ALS, DKB, MSC. Data collected by ALS, DKB, BMK. Data analyzed and interpreted by ALS, DKB, BMK, JCM, DLS, MSC, KMK. Manuscript was written by ALK and KMK and revised and approved by all authors. KMK takes responsibility for the integrity of the data analysis.

References

1. Marini JC, Forlino A, Bächinger HP, et al. Osteogenesis imperfecta. Nat Rev Dis Primers. 2017;3:17052.
2. Zeitlin L, Fassier F, Glorieux FH. Modern approach to children with osteogenesis imperfecta. J Pediatr Orthop. 2003;12:77–87.
3. Rauch F, Glorieux FH. Osteogenesis imperfecta. Lancet. 2004;363 (9418):1377–85.
4. Miller PD, Hattersley G, Riis BJ, et al. Effect of abaloparatide vs. placebo on new vertebral fractures in postmenopausal women with osteoporosis: a randomized clinical trial. JAMA. 2016;316(7): 722–33.
5. Neer RM, Arnaud CD, Zanchetta JR, et al. Effect of parathyroid hormone (1-34) on fractures and bone mineral density in postmenopausal women with osteoporosis. N Engl J Med. 2001;344(19): 1434–41.
6. Vahle JL, Sato M, Long GG, et al. Skeletal changes in rats given daily subcutaneous injections of recombinant human parathyroid hormone (1-34) for 2 years and relevance to human safety. Toxicol Pathol. 2002;30(3):312–21.
7. Jolette J, Attalla B, Varela A, et al. Comparing the incidence of bone tumors in rats chronically exposed to the selective PTH type 1 receptor agonist abaloparatide or PTH(1-34). Regul Toxicol Pharmacol. 2017;86:356–65.
8. Moester MJC, Papapoulos SE, Löwik CWGM, van Bezooijen RL. Sclerostin: current knowledge and future perspectives. Calcif Tissue Int. 2010;87(2):99–107.
9. Cosman FF, Crittenden DB, Adachi JD, et al. Romosozumab treatment in postmenopausal women with osteoporosis. N Engl J Med. 2016; 375(16):1532–43.
10. Sinder BP, Salemi JD, Ominsky MS, Caird MS, Marini JC, Kozloff KM. Rapidly growing Brtl/ mouse model of osteogenesis imperfecta improves bone mass and strength with sclerostin antibody treatment. Bone. 2015;71:115–23.
11. Roschger A, Roschger P, Keplingter P, et al. Effect of sclerostin antibody treatment in a mouse model of severe osteogenesis imperfecta. Bone. 2014;66:182–8.
12. Jacobsen CM, Barber LA, Ayturk UM, et al. Targeting the LRP5 pathway improves bone properties in a mouse model of osteogenesis imperfecta. J Bone Miner Res. 2014;29:2297–306.
13. Grafe I, Alexander S, Yang T, et al. Sclerostin antibody treatment improves the bone phenotype of Crtap mice, a model of recessive osteogenesis imperfecta. J Bone Miner Res. 2015;31(5):1030–40.
14. Cardinal M, Tys J, Roels T, et al. Sclerostin antibody reduces long bone fractures in the oim/oim model of osteogenesis imperfecta. Bone. 2019;124:137–47.
15. Sinder BP, White LE, Salemi JD, et al. Adult Brtl/+ mouse model of osteogenesis imperfecta demonstrates anabolic response to sclerostin antibody treatment with increased bone mass and strength. Osteoporos Int. 2014;25:2097.
16. Gardner J, VanBezooijen R, Mervis B, et al. Bone mineral density in sclerosteosis; affected individuals and gene carriers. J Clin Endocrinol Metab. 2005;90:6392–5.
17. Sharifi M, Ereifej L, Lewiecki EM. Sclerostin and skeletal health. Rev Endocr Metab Disord. 2015;16:149.
18. Wengenroth M, Vasvari G, Federspil PA, Mair J, Schneider P, Stippich C. Case 150: Van Buchem disease (hyperostosis corticalis generalisata). Radiology. 2009;253(1):272–6.
19. van Lierop AH, Appelman-Dijkstra NM, Papapoulos SE. Sclerostin deficiency in humans. Bone. 2017;96:51–62.
20. Kovero O, Pynnönen S, Kuurila-Svahn K, Kaitila I, Waltimo-Sirén J. Skull base abnormalities in osteogenesis imperfecta: a cephalometric evaluation of 54 patients and 108 control volunteers. J Neurosurg. 2006;105(3):361–70.
21. Davies MW, Inglis GD, Jardine LA, Koorts PJ. Antenatal Consults: A Guide for Neonatologists and Paediatricians. 1st ed. Sydney: Churchill Livingstone Elsevier; 2013.
22. Renaud A, Aucourt J, Weill J, et al. Radiographic features of osteogenesis imperfecta. Insights Imaging. 2013;4(4):417–29.
23. Semler O, Cheung MS, Glorieux FH, Rauch F. Wormian bones in osteogenesis imperfecta: correlation to clinical findings and genotype. Am J Med Genet. 2010;152A(7):1681–7.
24. Bellary S, Steinberg A, Mirzayan N, Shirak M, et al. Wormian bones: a review. Clin Anat. 2013;26:922–7.
25. Eimar H, Tamimi F, Retrouvey J-M, Rauch F, Aubin JE, McKee MD. Craniofacial and dental defects in the Col1a1Jrt/+ mouse model of osteogenesis imperfecta. J Dent Res. 2016;95(7):761–8.
26. De Carlos F, Varela I, Germana A, et al. Microcephalia with mandibular and dental dysplasia in adult Zmpste24-deficient mice. J Anat. 2008; 213(5):509–19.
27. Li X, Ominsky MS, Warmington KS, Morony S, et al. Sclerostin antibody treatment increases bone formation, bone mass, and bone strength in a rat model of postmenopausal osteoporosis. J Bone Miner Res. 2009;24:578.
28. Li X, Niu QT, Warmington KS, Asuncion FJ, et al. Progressive increases in bone mass and bone strength in an ovariectomized rat model of osteoporosis after 26 weeks of treatment with a sclerostin antibody. Endocrinology. 2014;155:4785.
29. Li X, Ominsky MS, Villasensor KS, et al. Sclerostin antibody reverses bone loss by increasing bone formation and decreasing bone resorption in a rat model of male osteoporosis. Endocrinology. 2018;159: 260–71.
30. Yao W, Dai W, Jiang L, et al. Sclerostin-antibody treatment of glucocorticoid-induced osteoporosis maintained bone mass and strength. Osteoporos Int. 2016;27:283.
31. Tian X, Jee WS, Li X, Paszty C, Ke HZ. Sclerostin antibody increases bone mass by stimulating bone formation and inhibiting bone resorption in a hindlimb-immobilization rat model. Bone. 2011; 48:197.
32. Spatz JM, Ellman R, Cloutier AM, Louis L, et al. Sclerostin antibody inhibits skeletal deterioration due to reduced mechanical loading. J Bone Miner Res. 2013;28:865.
33. Beggs LA, Ye F, Ghosh P, et al. Sclerostin inhibition prevents spinal cord injury-induced cancellous bone loss. J Bone Miner Res. 2015; 30:681.
34. Shah SA, Kormpakis I, Havlioglu N, et al. Sclerostin antibody treatment enhances rotator cuff tendon-to-bone healing in an animal model. J Bone Joint Surg Am. 2017;99:855–64.

35. McDonald MM, Morse A, Mikulec K, Peacookm L, et al. Inhibition of sclerostin by systemic treatment with sclerostin antibody enhances healing of proximal tibial defects in ovariectomized rats. J Orthop Res. 2012;30:1541.

36. Liu Y, Rui Y, Cheng TY, et al. Effects of sclerostin antibody on the healing of femoral fractures in ovariectomised rats. Calcif Tissue Int. 2016; 98:263.

37. Kozloff KM, Carden A, Bergwitz C, et al. Brittle IV mouse model for osteogenesis imperfecta IV demonstrates postpubertal adaptations to improve whole bone strength. J Bone Miner Res. 2004;19:614–22.

38. Uveges TE, Collin-Osdoby P, Cabral WA, et al. Cellular mechanism of decreased bone in Brtl mouse model of OI: imbalance of decreased osteoblast function and increased osteoclasts and their precursors. J Bone Miner Res. 2008;23:1983–94.

39. Forlino A, Marini JC. Osteogenesis imperfecta: prospects for molecular therapeutics. Mol Genet Metab. 2000;71(1–2):225–32.

40. Perosky JE, Khoury B, Jenks T, et al. Single dose of bisphosphonate preserves gains in bone mass following cessation of sclerostin antibody in Brtl/+ osteogenesis imperfecta model. Bone. 2016;93:79.

41. Takahashi H, Hitsumoto Y, Honda N, et al. Mouse model of Bells palsy induced by reactivation of herpes simplex virus type 1. J Neuropathol Exp Neurol. 2001;60(6):621–7.

42. Richtsmeier JT, Baxter LL, Reeves RH. Parallels of craniofacial maldevelopment in down syndrome and Ts65Dn mice. Dev Dyn. 2000; 217:137–45.

43. Bookstein FL, Chernoff B, Elder RL, Humphries J, Smith G, Strauss, R. Morphometrics in evolutionary biology: the geometry of size and shape change, with examples from fishes. Philadelphia, PA: Academy of Natural Sciences of Philadelphia, Special Publication No. 15 1985.

44. Bookstein FL. Morphometric tools for landmark data. Geometry and biology. Cambridge, UK: Cambridge University Press; 1991.

45. Bookstein FL. Standard formula for the uniform shape component in landmark data. In Marcus LF, Corti M, Loy A, Naylor GJP, Slice DE, eds. Advances in morphometrics. NATO Advanced Science Institutes Series, Series A, Life Sciences, vol. 284. New York: Plenum Press; 1996 pp 153–68.

46. Adams DC, Collyer ML, Kaliontzopolou A Sherrat E. Geomorph: software for geometric morphometric analysis. R package version 3.0.5; 2017 [Online]. Available from: http://cran.r-project.org/package=geomorph. Accessed January, 2018.

47. Thompson DAW. On growth and form. The Complete Revised Edition. 2nd ed. Dover; 1942 (reprinted 1992). Cambridge: Cambridge University Press.

48. Adams DC, Collyer ML. Analysis of character divergence along environmental gradients and other covariates. Evolution. 2007;61(3): 510–5.

49. Yoshimura K, Kobayashi R, Ohmura T, Kajimoto Y, Miura T. A new mathematical model for pattern formation by cranial sutures. J Theor Biol. 2016;408:66–74.

50. Byron CD, Borke J, Yu J, et al. Effects of increased muscle mass on mouse sagittal suture morphology and mechanics. Anat Rec A Discov Mol Cell Evol Biol. 2004;279:676–84.

51. Behr B, Longaker MT, Quarto N. Differential activation of canonical Wnt signaling determines cranial sutures fate: a novel mechanism for sagittal suture craniosynostosis. Dev Biol. 2010;344(2):922–40.

52. Miura T, Perlyn CA, Kinboshi M, et al. Mechanism of skull suture maintenance and interdigitation. J Anat. 2009;215(6):642–55.

53. Paxinos G. The rat nervous system. Amsterdam: Academic Press; 2015.

54. Greene EC. Anatomy of the Rat. New York: Hafner Pub Co.; 1963.

55. Gray H, Carter H. Anatomy of the Human Body. 20th ed. Philadelphia: Lea & Febiger; 1918.

56. Basivertebral foramen. Clinical Anatomy Associates, Inc. [Cited November 26, 2017]. Available from: https://clinanat.com/100-mtd/142-basivertebral-foramen.

57. Agholme F, Isaksson H, Li X, Ke HZ, Aspenberg P. Anti-sclerostin antibody and mechanical loading appear to influence metaphyseal bone independently in rats. Acta Orthop. 2011;82:628.

58. Olvera D, Stolzenfeld R, Marini JC, Caird MS, Kozloff KM. Low dose of bisphosphonate enhances sclerostin antibody-induced trabecular bone mass gains in Brtl/+ osteogenesis imperfecta mouse model. J Bone Miner Res. 2018;33(7):1272.

59. Little DG, Peacock L, Mikulec K, Kneissel M, et al. Combination sclerostin antibody and zoledronic acid treatment outperforms either treatment alone in a mouse model of osteogenesis imperfecta. Bone. 2017;101:96.

60. Beneke JE. Facial nerve dysfunction in osteopetrosis. Laryngoscope. 1993;103(5):494–7.

61. Benichou OD, Laredo JD, de Vernejoul MC. Type II autosomal dominant osteopetrosis (Albers-Schonberg disease): clinical and radiological manifestations in 42 patients. Bone. 2000;26(1):87–93.

62. Kozloff KM. Osteogenesis imperfecta: a need to understand divergent treatment outcomes in a disorder rich in heterogeneity. J Bone Miner Res. 2019;34(2):205.

63. Vora SR, Camci ED, Cox TC. Postnatal ontogeny of the cranial base and craniofacial skeleton in male C57BL/6J mice: a reference standard for quantitative analysis. Front Physiol. 2015;6:417.

64. Baldrick P. Developing drugs for pediatric use: a role of juvenile animal studies? Regul Toxicol Pharmacol. 2004;39:381–9.

65. Jin S, Sim K, Kim S. Development and growth of the normal cranial vault: an embryologic review. J Korean Neurosurg Soc. 2016;59(3): 192–6.